JOURNAL OF AGRICULTURAL AND FOOD CHEMISTRY

pubs.acs.org/JAFC Article

Structure of *In Vitro* Digestion Residues from High-Amylose Starch Impacts Colonic Microbial Composition and Metabolic Activity

Yu Tian, Yu Wang, Xinming Xu, Bekzod Khakimov, Xingxun Liu, Lude Zhang, Zhuqing Xie, Jacob J. K. Kirkensgaard, Kim H. Hebelstrup, Dennis S. Nielsen, Birte Svensson,* and Andreas Blennow*

Cite This: https://doi.org/10.1021/acs.jafc.6c06220 Read Online

ACCESS | Metrics & More | Article Recommendations | Supporting Information

ABSTRACT: Resistant starch (RS) is a nondigestible carbohydrate that serves as a prebiotic and is fermented by colonic bacteria to produce short-chain fatty acids (SCFAs). Here, *in vitro* digestion-derived residues (RSs) from five high-amylose starches (HASs; four RS2 and one RS3) were evaluated for their effects on microbiota composition and SCFA production using a simulated colonic fermentation model inoculated with human fecal microbiota. RSs with more amorphous structures and lower short-range order generated the highest SCFA levels and promoted the growth of the primary RS degrader *Bifidobacterium adolescentis*. In contrast, RSs with higher resistance to digestion and retained B-type crystallinity favored propionate-associated taxa, including *Veillonella* spp. and *Bacteroides* spp., whereas less resistant RSs promoted butyrate-producing taxa such as *Clostridium* spp. These results suggest that structural features of RS are associated with differences in microbial composition and metabolic activity, providing insights into the design of HAS-based dietary fibers with targeted prebiotic functions.

KEYWORDS: *high amylose starch, resistant starch, gut microbiota, simulated colonic fermentation, short-chain fatty acids*

1. INTRODUCTION

The gut microbiota play a fundamental role in maintaining human health by regulating various physiological functions, including metabolism, immune responses, and fat storage.[1−3] Diet is a critical factor in shaping the composition and activity of the gut microbiota, with particular emphasis on indigestible carbohydrates.[2,4,5] Starch is the major dietary carbohydrate consumed worldwide, and its digestion-resistant fraction, termed resistant starch (RS), has attracted considerable attention due to its prebiotic properties.[5,6]

The gut bacteria utilizing RS are categorized into primary degraders, directly decomposing RS enzymatically, and secondary degraders, or cross-feeders, utilizing the products of the primary degraders, like oligosaccharides and metabolites.[7−10] Key microbiota members, including strains of *Bifidobacterium adolescentis* and *Ruminococcus bromii*, are primary degraders of the complex and compact RS granules (native (RS2) and retrograded (RS3) structures),[11] enabling other gut bacteria to propagate on this type of substrate. Selected gut microbiota members are capable of fermenting RS and forming short-chain fatty acids (SCFAs), having different physiological effects and are widely considered beneficial.[12−15] Butyrate, for example, serves as an energy source for mucosal cells and is linked to protection against colorectal cancer, while propionate contributes to gluconeogenesis in the liver and has been associated with promoting satiety, lowering cholesterol, and maintaining glucose homeostasis.[16−18] The SCFA production in RS colonic fermentation relies on a syntrophic network of cross-feeding interactions. RS is broadly classified into five types (RS1−RS5) based on its structural origin: physically entrapped starch (RS1), native granular starch (RS2), retrograded starch (RS3), chemically modified starch (RS4), and amylose-lipid complexes (RS5).[6] These types exert distinct effects on gut microbiota composition and metabolic output.[9,19−21] Even different kinds of HAS of the same RS type can elicit exclusive responses. For instance, within the RS2 category, native corn HAS supplementation was associated with an increase in *R. bromii* and the butyrate-producer *Eubacterium rectale*, whereas native potato HAS primarily favored *B. adolescentis*, with an overall increase in SCFA production.[20]

Starch consists of two glucose polymers (α-glucans): the essentially linear amylose (AM) and the branched amylopectin (AP).[22] HAS granules have higher amylose (50−90%) relative to amylopectin content than normal starches and are an important source of RS.[23] Their structural features endow (i) fewer attack sites for hydrolytic enzymes on the granular surface and (ii) dynamic reorganization of AM and AP chains during digestion.[24,25] Several HAS crops are available, including wheat, maize, barley, potatoes, and peas.[26−29] Previous studies have shown that HASs from different sources exhibit distinct granular features, internal molecular reorganization capabilities, and resistance to digestive enzymes.[25,29,30] Moreover, starches differing in botanical origin and structural characteristics have been reported to affect gut microbiota composition and SCFA production differentially.[5] However, the upper gut digestion-induced reorganization generates RS

Received: April 27, 2026
Revised: July 31, 2026
Accepted: August 10, 2026

ACS Publications © XXXX American Chemical Society

residues with distinct crystalline and molecular features, which are biomimetically generated in this study. Hence, these digestion-derived RS fractions, rather than the native starches themselves, are the substrates that ultimately reach the colon and interact with gut microbiota. The relationships between the structural characteristics of digestion-derived RS fractions and their effects on microbial composition and metabolic activity remain poorly understood.

To better understand how structural differences among digestion-derived HAS-RS fractions influence gut microbiota composition and SCFA production, residual RS fractions were generated from five HASs using an *in vitro* digestion procedure.[25] The obtained individual HAS-derived RS fractions were isolated and subjected to simulated colonic fermentation at controlled temperature and pH[31] by fecal inocula from three healthy donors. Simulated colonic fermentation of the different *in vitro*-digested HAS RS substrates elicited differences in microbiota dynamics and SCFA profiles. The findings provide a foundation to understand and exploit HASs' potential for dietary interventions to enhance gut health.

2. MATERIALS AND METHODS

2.1. Materials

Four of the RSs were generated from native granular HASs, i.e., RS type 2,[32] of different crops showing assorted hydrolase resistance. A subgroup of RS3, referred to as enhanced resistant starch (eRS), was prepared by "amylolytic shaving" of amylose-only barley starch (AOBS) granules,[25] which was included as an amylolytically highly resistant model to extend the range of digestion-derived RS structures evaluated in this study. Specifically, four starches from high-amylose crops: maize, Hylon VII, Ingredion, USA, and NAFU60 from China, referred to as HAMSI and HAMSII with amylose content (AC) of 72% and 61%, respectively;[33] wheat with AC 67% (HAWS; gift of Northwest A&F University, China); and barley with AC 97% (amylose-only barley starch, AOBS).[27,34] To obtain enhanced RS (eRS), AOBS was treated with pancreatin (Sigma-Aldrich, P7545) and amyloglucosidase (Sigma-Aldrich, A7095) in a simulated intestinal digestion system (50 mM sodium acetate, 5 mM $CaCl_2$, pH 5.5, 37 °C) for 10 h under gentle agitation, as previously described.[25] The reaction was terminated by adding Na_2CO_3 (0.3 M resulting concentration), and the AOBSeRS, regarded as RS3, was washed and freeze-dried.

2.2. *In Vitro* Enzymatic HAS Digestion

Prior to the simulated colonic fermentation (see Section 2.4), the HASs were subjected to a standardized static *in vitro* biochemical salivary, gastric, and intestinal digestion model.[26,35] Buffers for SSF, SGF, and SIF fluids were prepared and adjusted to pH 7.0, 3.0, and 7.0, respectively, as described in Supporting Information. Five grams of HAS were mixed with 5 mL of SSF with 375 U salivary amylase (Sigma-Aldrich, A1031) and incubated for 2 min at 37 °C with orbital agitation. After the oral phase, 10 mL of SGF with 20,000 U pepsin (Sigma, P7000, from porcine gastric mucosa) was added, and the pH was adjusted to 3.0 with 0.1 M HCl, followed by incubation for 2 h at 37 °C with orbital agitation. Finally, for the intestinal phase, 20 mL of SIF with 2000 U pancreatin (Sigma-Aldrich, P7545) and 10 mM bile salts (Sigma-Aldrich, B8631) werer added, and the pH was adjusted to 7.0 with 0.1 M NaOH, followed by 2 h of incubation with orbital agitation at 37 °C. The "0 time" aliquot (50 μL) was collected before the addition of SIF. Subsequent aliquots (50 μL) were removed at different time points and mixed with 0.5 M Na_2CO_3 (450 μL) to stop amylolytic hydrolysis, and the sample wascentrifuged (2,000 *g*, 10 min). Digested starch (%) was calculated from the released reducing sugar, determined using a 4-hydroxybenzoic acid hydrazide (PAHBAH) method and maltose as the standard (absorbance measured at 405 nm).[24,36] Rapidly digested starch (RDS) and slowly digested starch (SDS) were defined as starch hydrolyzed within the first 20 min, and during 20−120 min, respectively; RS was the precipitate obtained after 120 min.[37] The amounts of RDS, SDS, and RS were calculated based on the total starch content and released reducing sugars at specific time points. After 120 min of intestinal phase digestion, the reaction was stopped by the addition of Na_2CO_3 (0.3 M final concentration). The resulting suspension was transferred to 50 mL Falcon tubes and centrifuged (2,000 *g*, 10 min). The sediment, corresponding to the RS fraction, was collected, washed three times with Milli-Q water, freeze-dried, and used for simulated *in vitro* colonic fermentation (see Section 2.4).

2.3. Crystallinity, Degree of Surface Order, and Morphological Observation

The digestion-derived RS fractions obtained after 120 min of *in vitro* digestion (see Section 2.2) were analyzed for crystallinity, degree of surface order, and morphology.[34] Crystal structures were analyzed using a Nano-inXider instrument (Xenocs SAS, Grenoble, France) after conditioning the RS samples with saturated KCl for 72 h in a humidity chamber. The relative crystallinity was calculated using the PeakFit software (version 4.12, Systat Software, Inc., San Jose, CA, USA) following the estimation of the amorphous background scattering as described.[25] The crystalline polymorphs were identified based on the characteristic diffraction peaks and corresponding 2θ angles.[38] The degree of surface order was estimated by Fourier transform infrared (FTIR) spectroscopy using a Bomem MB100 FTIR spectrometer equipped with a Golden Gate attenuated total reflectance (ATR) accessory.[39] Spectra were collected at a resolution of 4 cm^{-1} and coadded for each sample. Background spectra were obtained by cleaning the crystal with a mixture of ethanol and water and recording 64 coadded scans. A Lorentzian line shape with a half-width of 19 cm^{-1} and a resolution enhancement factor of 1.9 was assumed. Baseline correction and deconvolution analysis were performed using the OMNIC software. IR absorbance values at 1022 cm^{-1} and 1045 cm^{-1} were extracted from the spectra, and the 1045 cm^{-1}/1022 cm^{-1} absorbance ratio was determined. The morphology of the starch granules was monitored by field emission scanning electron microscopy (FE-SEM, FEI Quanta 200) after fixing and sputter-coating the granules with gold.[34]

2.4. *In Vitro* Simulated Colonic Fermentation

The effects of the five RSs prepared as described (see Section 2.2) and inulin (positive control) on gut microbiota composition were investigated using an *in vitro* simulated colonic passage model (the CoMiniGut), which allowed for temperature control and dynamic control of pH over a 24-h fermentation period.[31] Inulin was selected as a positive control because it is a well-established, highly fermentable prebiotic fiber commonly used in gut microbiota fermentation studies.[4] Fecal samples were collected from three healthy adult donors (1 female and 2 males; age range 25−35 years) who had no known gastrointestinal disease and had not taken antibiotics or probiotics within the last six months. The study was approved by the Ethical Committee of the Capital Region of Denmark (registration number H-20028549). Individual stool samples were transferred to the anaerobic chamber within minutes after collection and homogenized with sterilized PBS/20% glycerol (v/v) at a ratio of 1:1 for 120 s using the Stomacher (Stomacher 400; Seward, Worthing, UK). The glycerol stocks were aliquoted into cryovials and stored at −60 °C before use as fecal inoculum for the fermentations.

The basal medium used for simulated colonic fermentation included 0.5 g/L bile salts, 1.5 g/L peptone water, 1.0 g/L yeast extract (Oxoid), 1.0 g/L porcine mucin (Sigma-Aldrich, Steinheim, Germany), 0.1 g/L NaCl, 0.04 g/L K_2HPO_4, 0.04 g/L KH_2PO_4 (Merck, Kenilworth, NJ), 0.01 g/L $MgSO_4{\cdot}7H_2O$, 0.01 g/L $CaCl_2{\cdot}6H_2O$, 2 g/L $NaHCO_3$, 0.002 g/L hemin, 10 μL/L vitamin K_1, 2 mL Tween-80 (Sigma-Aldrich), and 0.5 g/L L-cysteine HCl (Calbiochem, San Diego, CA). Prior to fermentation, 50 mg RS or inulin was dispersed (RS) or dissolved (inulin) in 4.5 mL basal medium directly. Each CoMiniGut reactor was filled with 0.5 mL fecal sample and 4.5

https://doi.org/10.1021/acs.jafc.6c06220
J. Agric. Food Chem. XXXX, XXX, XXX−XXX

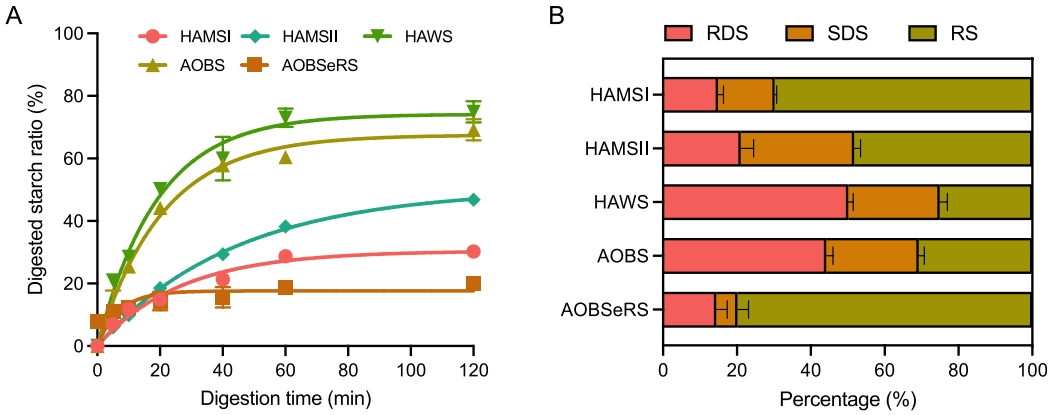

Figure 1. Intestinal *in vitro* digestion profiles of five HASs (A) and their RDS, SDS, and RS contents (B). High-amylose maize starches: HAMSI, HAMSII; high-amylose wheat starch: HAWS; amylose-only barley starch: AOBS; AOBS-enhanced resistant starch: AOBSeRS. Amylose contents are given in the Materials and methods Section 2.1.

Table 1. Crystalline Structure and Short-Range Order of Different RSs

	Crystallinity (%)		B-type crystallinity (%)		Surface order degree (1045 cm^{-1}/1022 cm^{-1})	
Sample	Before[i]	After[ii]	Before	After	Before	After
HAMSI	22.0 ± 0.7[iii a]	23.5 ± 0.7[a]	18.0 ± 0.4[a]	19.4 ± 0.7[a]	0.54 ± 0.01[b]	0.72 ± 0.05[b]
HAMSII	21.8 ± 2.8[a]	16.8 ± 0.1[b]	18.8 ± 2.7[ab]	11.9 ± 0.1[ab]	0.50 ± 0.05[c]	0.55 ± 0.05[c]
HAWS	10.2 ± 1.2[b]	12.4 ± 1.1[b]	8.4 ± 0.6[b]	9.2 ± 0.3[b]	0.38 ± 0.01[c]	0.59 ± 0.01[c]
AOBS	13.8 ± 0.3[b]	15.4 ± 0.2[b]	4.8 ± 0.3[b]	6.6 ± 0.1[b]	0.10 ± 0.05[c]	0.45 ± 0.04[c]
AOBSeRS	20.5 ± 3.6[a]	21.5 ± 1.5[a]	18.5 ± 2.4[a]	19.6 ± 1.5[a]	1.40 ± 0.23[a]	1.28 ± 0.10[a]

[i]Before: native HAS. [ii]After: RS derived from HAS after 120 min of intestinal *in vitro* digestion. [iii]The values of mean ± SD for all parameters were calculated from duplicate measurements. Values with different letters in the same column are significantly different at $p < 0.05$. Abbreviations are as in Figure 1.

mL basal medium containing either the specific RS or inulin, resulting in a final concentration of 10 mg/mL. Anaerobic fermentation was conducted with stirring at 37 °C for 24 h. The pH was continuously monitored and adjusted to simulate different sections of the colon: pH 5.7−6.0 for the proximal colon (first 8 h), pH 6.0−6.5 for the transverse colon (8 h), and pH 6.5−6.9 for the distal colon (final 8 h). The pH profiles of the inulin and HAS-RS fermentations with pH control are displayed in Figure S1. Substrate (RSs or inulin) was fermented in duplicate for each of the three donors, resulting in six fermentations per substrate. After the 24 h fermentation period, the slurry was collected and stored at −80 °C for further analysis. Inulin served as the positive control, and blank controls consisted of the fecal inoculum from each donor in 4.5 mL of basal medium without any added carbohydrate substrate. The variation in responses among the donors was maximized by not pooling the three fecal samples. The use of individual donor slurries aimed to increase the reliability of detecting changes induced by the starch samples during fermentation.[40]

2.5. DNA Extraction, 16S rRNA Gene Amplicon Sequencing, Bioinformatics, and Phylogenetics

The microbiota composition of each fermented sample was determined using near-full-length 16S rRNA gene amplicon sequencing on the Oxford Nanopore GridION X5 platform (Oxford Nanopore Technologies, Oxford, United Kingdom), as previously described.[41] DNA was extracted from each sample using the BeadBeat Micro AX Gravity Kit (A&A Biotechnology, Gdynia, Poland). The purity and concentration of DNA were verified using a NanoDrop 1000 Spectrophotometer (Thermo Fisher Scientific) and quantified with a Qubit 1× dsDNA high-sensitivity kit on a Varioskan Flash (Thermo Fisher Scientific). The construction of the 16S rRNA gene amplicon library and sequencing data collection followed previously established protocols.[41]

α-diversity, specifically the Shannon Richness Index, was calculated based on Shannon−Wiener diversity. The microbial composition was analyzed and visualized using stacked columns and heatmaps through the R package ampvis2.[42]

To assess the effects of the different RS samples, duplicate fermentations from each donor−substrate combination were first averaged, and the resulting donor-specific means were used as biological replicates (n = 3 donors). Results are presented as average values across the three donors. The response data averages from the five RS substrates, inulin, and blank controls were then compared. For clarity, results were presented as relative abundances and analyzed at the phylum, family, genus, and species levels.

2.6. Short-Chain Fatty Acids (SCFAs) Analysis

SCFA profiles were extracted from 1 mL of fermentation samples. Two milliliters of 0.3 M oxalic acid was added to each sample, vortexed for 1 min, and followed by centrifugation (3,000 *g*, 15 min). The SCFAs in the supernatants were identified and quantified by gas chromatography−mass spectrometry (GC-MS), as previously described[31] using formic, acetic, propionic, and butyric acids (Sigma-Aldrich) as standards. For SCFA analysis, duplicate fermentations from each donor were first averaged, and the resulting donor-specific means were used as biological replicates (n = 3 donors) for each substrate. Spearman correlation between SCFA content and microbiota composition at the genus level was analyzed and visualized using the R package Rhea.[43]

2.7. Statistical and Clustering Analyses

Structural and digestion data (Figure 1 and Table 1) are expressed as mean ± standard deviation. Statistical analyses were performed using SPSS 26.0 (IBM Corp., Armonk, NY, USA). One-way analysis of variance (ANOVA), followed by Duncan's multiple range test, was conducted to determine significant differences among samples, with a significance level set at $p < 0.05$.

https://doi.org/10.1021/acs.jafc.6c06220
J. Agric. Food Chem. XXXX, XXX, XXX−XXX

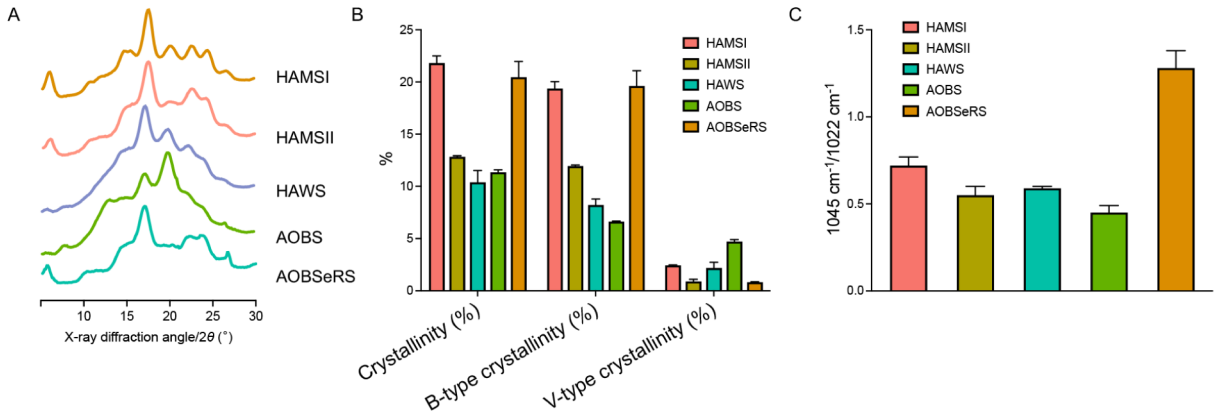

Figure 2. X-ray diffraction (XRD) patterns of different RSs (after 120 min of HASs *in vitro* digestion) (A), their relative crystallinity as deduced from XRD (B), and surface order degree as determined by FTIR (C). Abbreviations are as in Figure 1.

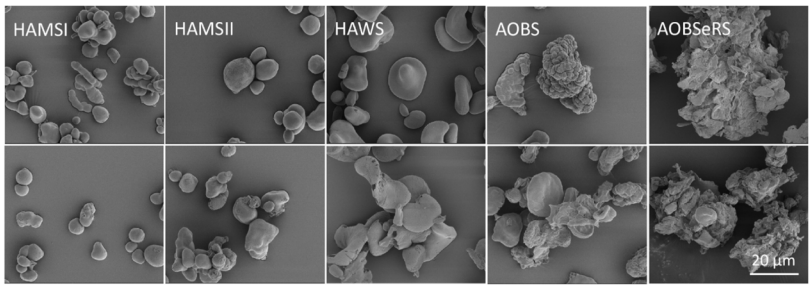

Figure 3. Scanning electron microscopy (SEM) images of native high-amylose starches (HAS; upper panel) and their corresponding resistant starch (RS) residues (lower panel) obtained after 120 min *in vitro* intestinal digestion. Abbreviations are as in Figure 1.

All statistical analyses of microbiota and SCFAs (Figures 4–8) were conducted using R software (version 4.4.1) via RStudio. To compare the relative abundance of microbiota changes in two RS groups (see Section 3.4.3 for group definitions), organisms with differences in response to each RS group were identified using one-tailed paired Wilcoxon tests on the average abundances in each subject before and after supplementation. Spearman correlations were calculated between *B. adolescentis* and other key taxa in each of the two RS groups. All *p*-values were corrected with the Benjamini–Hochberg method.[9,26]

3. RESULTS

3.1. Salivary, Gastric, and Intestinal *In Vitro* Digestibility Analysis

Following the SSF and SGF treatments, the intestinal *in vitro* digestion profiles and RDS, SDS, and RS contents of the five HASs (Figure 1) demonstrated that all examined HASs exhibited a high RS content (>25%), in agreement with a previous study.[25] However, distinct variation in the extent of hydrolytic resistance was observed. HAMSI and AOBSeRS were the least digestible and most resistant to hydrolysis (70–80%), while HAMSII, AOBS, and HAWS showed higher digestibility and lower resistance (25–50%) (Figure 1B).

3.2. Structural Characterization of the Different Resistant Starches

The utilization of the RSs by human gut microbiota is closely related to their structure.[44] The five RSs obtained after 120 min *in vitro* digestion (see Section 2.2 and Figure 1A) and used as substrates in the simulated colonic fermentation (see Section 2.4) were structurally characterized. First, the crystalline structures of the RSs exhibited a combination of B-type (with 2θ angle peaks at 5.6°, 15°, 17°, 22°, 24°, and 26°) and V-type (with peaks at the 2θ angles 8°, 13°, 15°, and 20°) crystalline polymorphs (Figure 2).[45] RSs of HAWS and AOBS showed 1.1- and 1.2-fold higher crystallinity, respectively, after *in vitro* intestinal digestion than their native HAS counterparts, indicative of molecular reorganization, particularly leading to the B-type polymorph (Table 1). However, HAWS and AOBS reorganized to a lower degree and showed the lowest crystallinity (15.4% and 12.4%) among the five RS samples. In contrast, HAMSI and AOBSeRS maintained almost unchanged crystal structures after the digestion and the highest portion (20%) of the B-type crystalline polymorph.

The degree of surface order among the five HASs, as estimated by the 1045 cm^{-1}/1022 cm^{-1} ratio in FTIR spectra, was highest for AOBSeRS (1.28), followed by HAMSI (0.72) (Table 1; FTIR spectra are shown in Figure S2). Notably, although HAWS and AOBS gained 1.6- and 4.5-fold increase in the degree of surface order after 120 min *in vitro* digestion, it was still lower than for HAMSI and AOBSeRS. Finally, HAMSII exhibited a relatively stable surface structure, as indicated by a similar degree of surface order (0.50 and 0.55) before and after *in vitro* digestion (Table 1).

All five RSs maintained their granular structure and surface morphology after 120 min *in vitro* digestion, as determined by field emission scanning electron microscopy (FE-SEM) (Figure 3). The appearance of small pores on the relatively smooth surface was observed in HAMSI granules. AOBSeRS granules exhibited a highly reorganized structure of small granules aggregated into "sheaths" which appeared to present the most resistant structure (Figure 1).[46] HAMSII displayed larger pores on the surface, while HAWS and AOBS granules showed a mixture of broken and reorganized granules.

https://doi.org/10.1021/acs.jafc.6c06220
J. Agric. Food Chem. XXXX, XXX, XXX−XXX

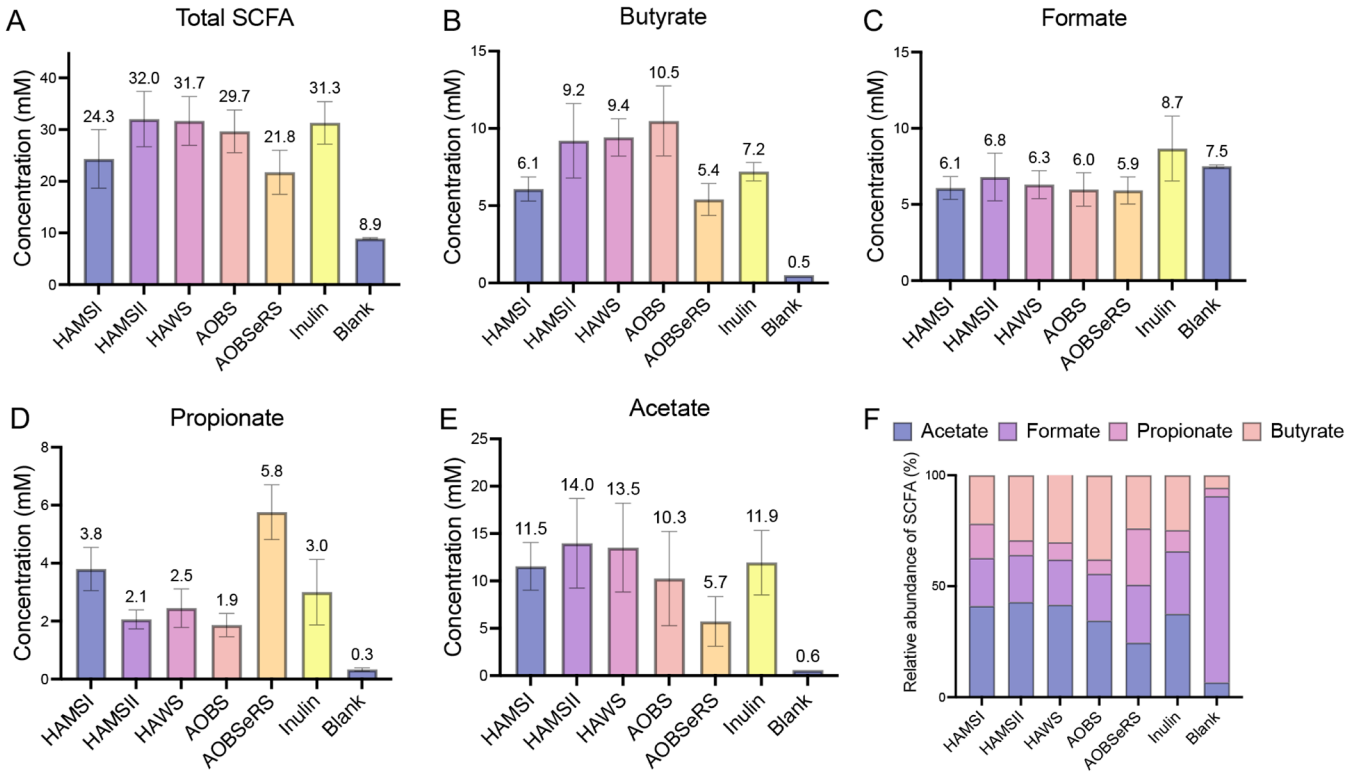

Figure 4. Concentrations of produced short-chain fatty acids (SCFAs) in fecal slurries after simulated colon fermentation by human fecal inocula (A); butyrate (B); formate (C); propionate (D); acetate (E) of each fermented sample; and the relative abundance of the SCFAs (F). Data are presented as means of three donor-specific values (n = 3 biological replicates), with duplicate fermentations averaged within each donor. Abbreviations are as in Figure 1.

Overall, after 120 min of *in vitro* digestion, HAMSI and AOBSeRS, due to their inherently well-organized structures, largely retained their crystallinity, degree of surface order, and morphology, presenting a highly resistant material available for passage to microbial fermentation in the colon.

3.3. Effects of RSs on Short-Chain Fatty Acid Production

The RS substrates resulted in distinctly different short-chain fatty acid (SCFA) profiles during the 24 h simulated colonic fermentation using the CoMiniGut (Figure 4). Notably, RSs and inulin (positive control) both increased the production of SCFAs by 2−3 times compared to blank controls (Figure 4A). Among the substrates, RSs originating from HAMSI and AOBSeRS led to relatively low concentrations of total SCFAs, indicating less fermentability for these RSs.

The relative proportions of SCFAs generated by fecal fermentation were nearly identical across the different RS treatments. All samples exhibited 10−20 times higher concentrations of acetate, butyrate, and propionate compared to the blank control, with levels comparable to or exceeding those observed for inulin (Figure 4B,D,F). However, compared to the blank control and inulin, the relative levels of formic acid were substantially lower in all fermented RS samples (Figure 4C). Formic acid is a common intermediate in colonic fermentation, and its lower accumulation suggests rapid utilization or diversion into alternative metabolic pathways by the microbiota when complex starches are provided.[6] Generally, HAMSI and AOBSeRS, having the highest RS contents (Figure 1), led to the release of lower levels of acetate and butyrate, but clearly higher levels of propionate compared to the less resistant substrates (HAMSII, HAWS, and AOBS) (Figure 4). The relative levels of butyrate were 20−23% for HAMSI and AOBSeRS, compared to 30−40% in the other three RS fermentations (Figure 4E).

Both butyrate and propionate are considered health-beneficial, although they influence host physiology differently.[17,20,47] Indeed, the present SCFA data clearly document that RSs, which possess variations in structural order and degradative resistance, have the capability to offer distinctly different prebiotic benefits via modulation of the microbiotal SCFA profiles.

3.4. Effects on the Bacterial Community

3.4.1. Shannon Richness Index. The α-diversity of the microbiota, as measured by the Shannon richness index, decreased after the fecal fermentation using CoMiniGut for all RS samples and inulin compared to the blank control (inoculum, no fermentation) (Figure 5). This decrease was expected, given that the inocula represent fecal microbiota previously exposed to a diverse human diet, while the fermented fecal slurries were subjected to a single carbohydrate source, either RS or inulin. Among the RSs, AOBS exhibited the lowest Shannon richness index of 3.3 (Figure 5). The reduction in α-diversity does not imply that RSs or inulin caused the death of specific microbial species but rather demonstrates that only certain bacteria are able to metabolize these carbon sources leading to their dominance.[48]

3.4.2. Changes at the Phylum Level. The predominant bacterial phyla were *Firmicutes* (recently renamed as *Bacillota*), *Bacteroidetes* (now *Bacteroidia*), and *Actinobacteria* (now *Actinomycetota*) (Figure 6). All five RSs and inulin increased the relative abundance of *Bacteroidetes* while decreasing *Firmicutes* compared with the blank control. Consequently, the *Bacteroidetes*-to-*Firmicutes* ratio increased for HAS-derived

https://doi.org/10.1021/acs.jafc.6c06220
J. Agric. Food Chem. XXXX, XXX, XXX−XXX

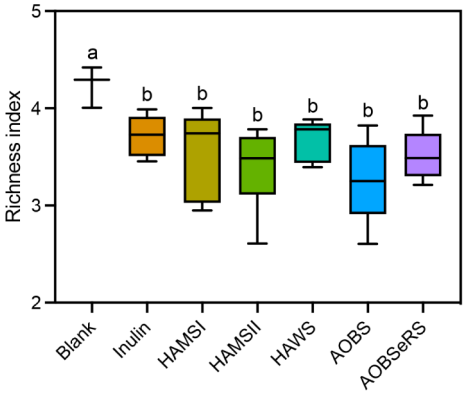

Figure 5. Shannon richness index of the microbial community of each *in vitro* simulated colonic microbiota when exposed to the RS substrates. Data are presented as means of three donor-specific values (n = 3), with duplicate fermentations averaged within each donor. Different lowercase letters indicate significant differences among samples at $p < 0.05$, as determined by one-way ANOVA followed by Duncan's multiple range test. Abbreviations are as in Figure 1.

RS substrates generated by *in vitro* intestinal digestion. *Firmicutes* and *Bacteroidetes* together constitute the majority of the gut microbiota. *Bacteroidetes* increased after fermentation of all RSs and inulin[49] and most so as being observed for AOBSeRS. On the basis of previous reports, *Bacteroides* members are known to possess diverse carbohydrate-active enzymes (CAZymes), which may contribute to their ability to utilize complex starch-derived substrates.[50] The *Actinobacteria* phylum includes the family *Bifidobacteriaceae*, encompassing a diverse array of specialized enzymes for carbohydrate utilization.[14] Notably, RSs derived from the most resistant HAMSI and AOBSeRS gave relatively lower increases in *Actinobacteria*.

3.4.3. Changes at the Species Level. A detailed investigation at the species level showed that, for all RS substrates, the relative abundance of *Bacteroides* spp., *Bifidobacterium adolescentis*, *Coprococcus comes*, *Prevotella copri*, and *Veillonella* spp. increased, and for *Dorea longicatena*, *Parabacteroides merdae*, and *Faecalibacterium* spp., the relative abundance decreased compared to the blank (Figure 7A,B). These data are in line with previous human dietary intervention studies, showing that the species mentioned above are also found to increase in the gut following the consumption of RS-containing diets.[20,51,52]

Considering the structural features of RSs (Figure 2), microbial abundance shifts, and impacts on SCFA production (Figure 4), we categorized the RSs into two groups (Figure 7C): Group 1, HAMSI and AOBSeRS, induced the formation of propionate; and Group 2, HAMSII, HAWS, and AOBS, led to higher butyrate production (Figure 4D,E). The major bacterial species that showed significantly different changes in abundance between the two groups are indicated in Figure 7C with a star. *Bacteroides* spp., *Parabacteroides* spp., and *Prevotella copri* increased on RSs of Group 1, whereas *Bifidobacterium* spp., *Clostridium* spp., *Coprococcus comes*, and *Megasphaera elsdenii* exhibited higher increase levels on Group 2 RSs.

Ruminococcus bromii and *Bifidobacterium adolescentis* are widely regarded as primary RS degraders in the human gut.[7] Among the HAS-derived RSs of group 2, HAMSII, HAWS, and AOBS showed a relatively higher increase in *Bifidobacterium* spp., while RSs derived from HASs in group 1, HAMSI and AOBSeRS, led to a lower increase in *Bifidobacterium* spp. compared to the blank control (Figure 7C).

The initial degradation of RS by primary degraders produces malto-oligosaccharides and simultaneously modifies the granule surface to allow degradation by nonprimary degraders.[11,53] By increasing the susceptibility of granular starch substrates, primary degraders enable secondary species to bind to and utilize a nutrient niche that was previously inaccessible in its native state.[7] Secondary degraders typically produce butyrate;[7] *Clostridium* spp. accordingly showed increased abundance when RSs from HAMSII and AOBS were used as the substrate, but the relative abundance of these species decreased in the AOBSeRS RS fermentations (Figure 7B), indicating different substrate preferences for *Clostridium* spp.[7] Besides, the positive relationship between *Clostridium* spp. and *Bifidobacteria* indicates a potential reliance on primary

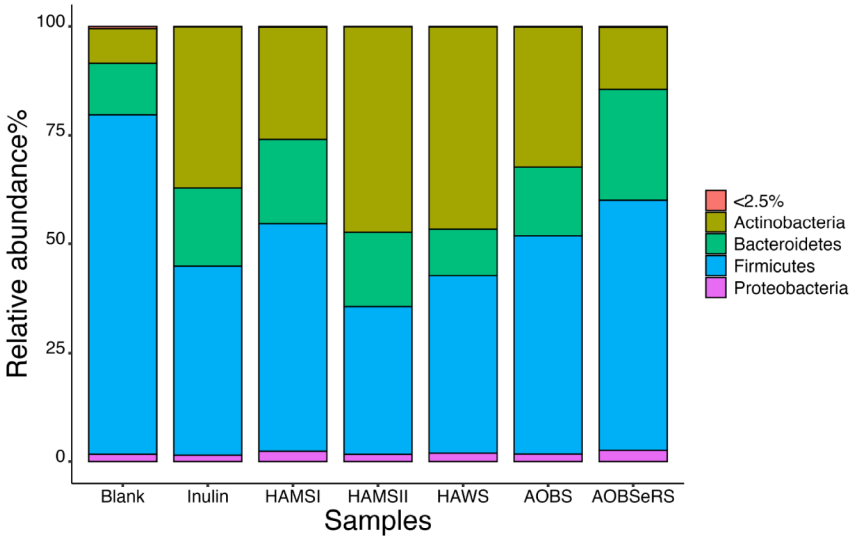

Figure 6. Relative abundance of the main phyla (>2.5%) in the *in vitro* simulated colonic microbiota when exposed to the RS substrates. Data are presented as means of three donor-specific values (n = 3 biological replicates), with duplicate fermentations averaged within each donor. Abbreviations are as in Figure 1.

https://doi.org/10.1021/acs.jafc.6c06220
J. Agric. Food Chem. XXXX, XXX, XXX−XXX

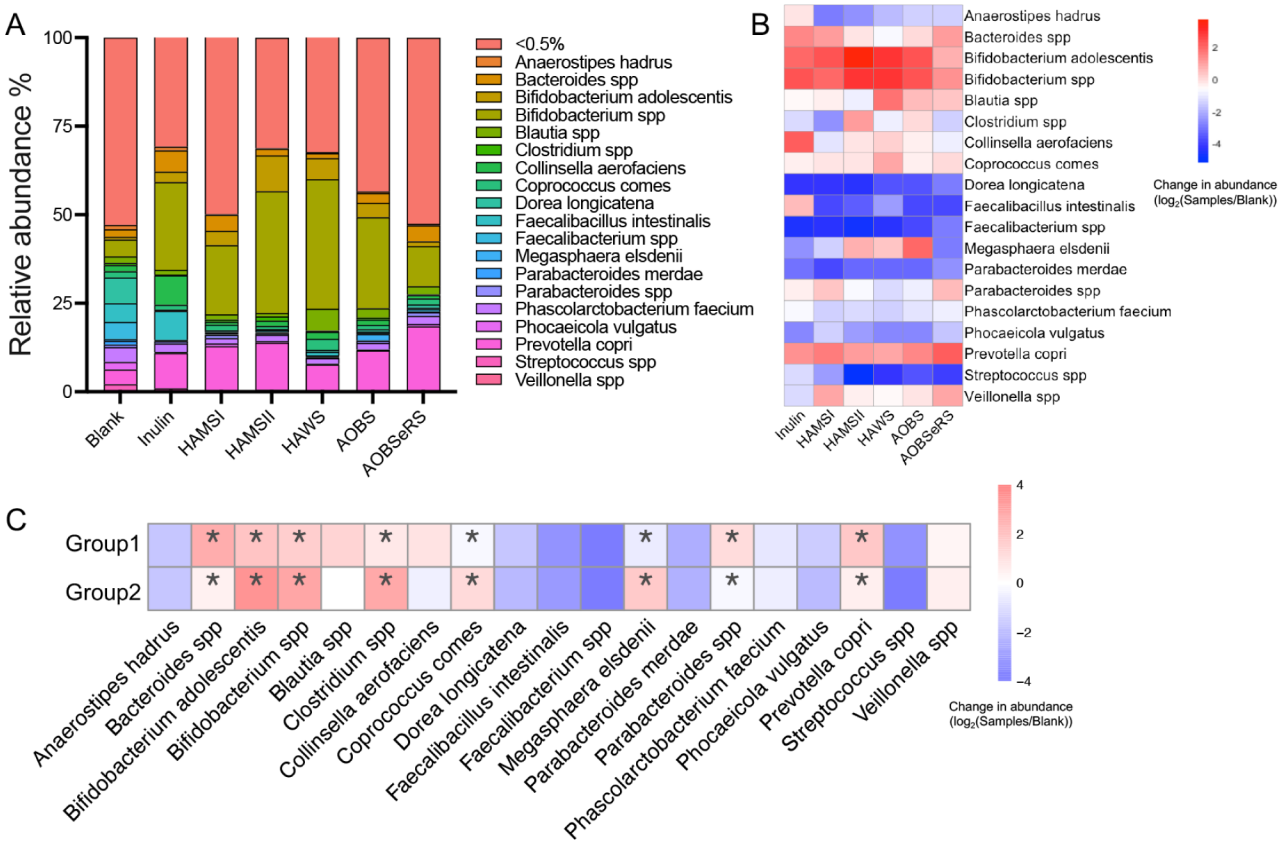

Figure 7. Relative abundance of the main species (>0.5%) of the microbiota in simulated colonic fermentation of the RS substrates. Data are presented as means of three donor-specific values (n = 3 biological replicates), with duplicate fermentations averaged within each donor (A); average fold change in the relative abundance of each species compared to the blank. The heatmap is colored by the standardized change in the relative abundance of the species between the treatment and the control. Red indicates a relative increase; blue indicates a relative decrease (B). The comparison panels are divided into two groups: group 1, including RS substrates leading to higher levels of propionate (HAMSI, AOBSeRS), and group 2, including RS substrates associated with higher levels of butyrate (HAMSII, HAWS, AOBS) (C). Significant differences between groups 1 and 2 were calculated using the paired Wilcoxon test; * indicates a significantly different change ($p < 0.05$) in the abundance of species between the two groups.

degraders for efficient RS erosion.[14] Fermentation of RS from HAWS showed the highest increase in *Coprococcus comes*, which has been demonstrated as a butyrate-producing bacterium through the phosphotransbutyrylase/butyrate kinase route.[54] *Megasphaera elsdenii* is also known to form butyrate in carbohydrate fermentation, but by utilizing acetate and lactate as key metabolic substrates.[39] This species was increased by RSs of group 2, especially AOBS.

Group 1 RSs gave a relatively higher increase in *Bacteroides* spp. compared with the other group. Besides, among the different RSs tested, AOBSeRS led to the highest increase in *Prevotella copri*. *Prevotella* belongs to the *Bacteroidetes* phylum and produces propionate through a succinate pathway. It includes major contributors to human gut enterotypes and is a critical functional phylotype correlated with high fiber intake.[55−57] Also, the genus *Parabacteroides* spp. increased in Group 1 RS fermentations and is considered a potential starch degrader with acetate and propionate as end products.[58] *Veillonella* spp., which increased for all RSs, especially HAMSI and AOBSeRS, can also produce propionate via the succinate pathway.[59]

3.5. Distinct Correlations of Different SCFAs and Bacterial Species

Correlation analysis between SCFA production and changes in bacterial relative abundance at the species level identified taxa associated with butyrate- or propionate-enriched fermentation profiles (Figure 8A). This aligned with previous data showing clear separation between butyrate- and propionate-producing bacteria, with only a few taxa exhibiting pathways for the production of both SCFAs.[59]

Propionate concentrations were positively correlated with increased abundances of *Blautia* spp., *Coprococcus comes*, *Collinsella aerofaciens*, *Parabacteroides* spp., and *Veillonella* spp. (Figure 8A). Some of these taxa have previously been linked to propionate formation, including succinate-associated pathways,[55] but the pathway activity was not directly assessed in this study. In contrast, the formation of butyrate correlated positively with *Bifidobacterium* spp., *Clostridium* spp., *Coprococcus comes*, *Megasphaera elsdenii*, and *Prevotella copri*. Furthermore, the fermentation of RS by *Bifidobacteria* yielded large quantities of acetate, as indicated by positive relationships (Figure 8A). Acetate can be metabolized into butyrate by other species.[60]

Bifidobacteria do not produce butyrate or propionate, as no such metabolic pathways are present in their genomes, despite a strong positive correlation with changes in butyrate concentration and *Bifidobacteria* (Figure 8A) due to a syntrophic cross-feeding mechanism, in which *Bifidobacteria* ferment RS into acetate and lactate; these metabolites then serve as essential substrates for secondary degraders (such as

https://doi.org/10.1021/acs.jafc.6c06220
J. Agric. Food Chem. XXXX, XXX, XXX−XXX

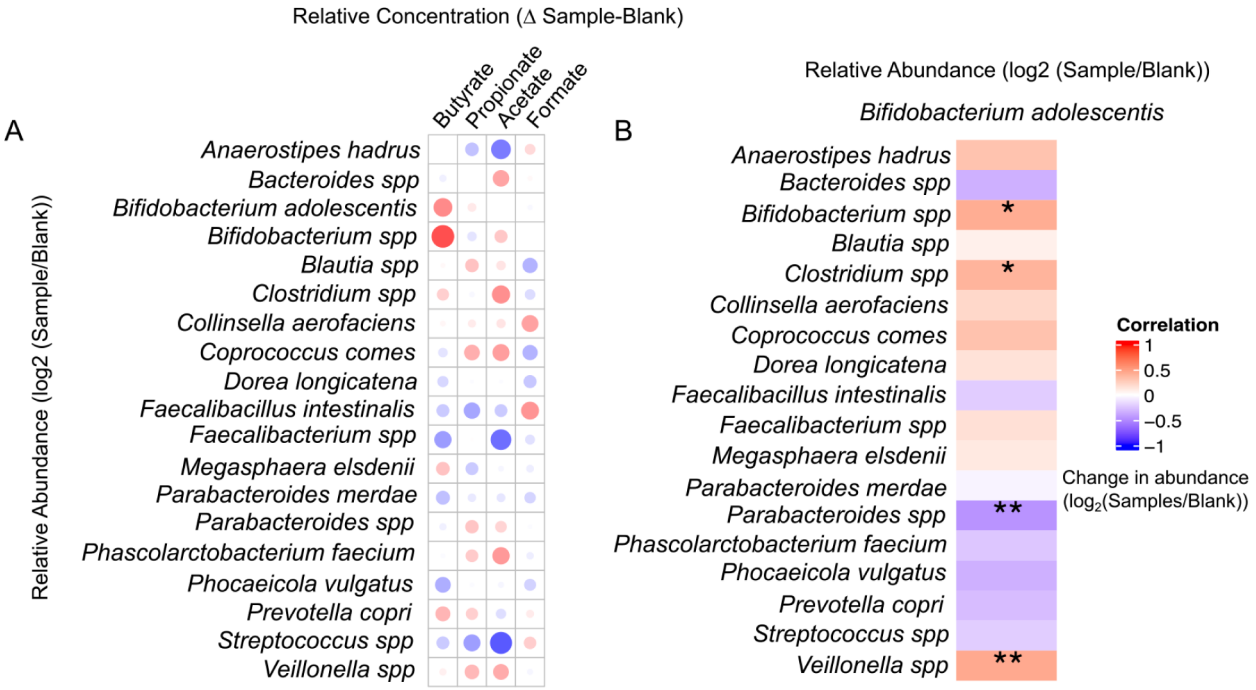

Figure 8. Spearman correlation between gut microbiota changes at the species level of the *in vitro* simulated colonic fermentation of RS substrates and changes in the major short-chain fatty acids—acetic acid, formic acid, propionic acid, and butyric acid (A). Spearman correlations were calculated using donor-specific values after averaging duplicate fermentations within each donor. The size of the circles represents the absolute value of the correlation coefficient, with larger circles indicating stronger correlations. Spearman correlations between changes in the abundance of the primary degrader (*B. adolescentis*) and other organisms (*$p < 0.05$, **$p < 0.01$) (B).

Clostridium spp.) to produce butyrate.[61] Positive correlations were observed between the primary RS degrader, *Bifidobacterium adolescentis* and butyrate-producing bacteria like *Clostridium* spp., as well as propionate-producing bacteria such as *Veillonella* spp. (Figure 8B).

4. DISCUSSION

4.1. Structure of HAS-RS Impacts *In Vitro* Fermentation Efficiency

HASs are widely recognized as a prominent source of RS2. As shown in our structural analysis, dynamic reorganization during *in vitro* intestinal digestion results in residual RSs with distinct physical and structural properties that are presumed to reach the colon. The inherently well-organized HAS granules of group 1 (HAMSI and AOBSeRS), characterized by higher B-type crystallinity and surface order (Table 1), present a more compact substrate for colonic fermentation compared to the more amorphous structures found in Group 2.

While all examined RS types were fermentable, the higher total SCFA concentrations from Group 2 indicate a superior fermentation efficiency for these less organized substrates. This observation aligns with previous findings that amorphous starch fractions allow broader enzymatic access, facilitating a more rapid conversion into metabolites.[21] However, this rapid fermentation does not necessarily equate to improved colonic health; the lower fermentation efficiency observed for Group 1 (AOBSeRS and HAMSI) suggests these starches may act as "slow-release" substrates. Such resistance can ensure that fermentable carbohydrates remain available for the microbiota in the distal colon, potentially preventing proteolytic fermentation (the degradation of proteins into potentially harmful metabolites) and supporting healthy metabolic activity across the entire colonic passage.[9]

Primary degraders are essential for initiating the breakdown of granular RS, releasing intermediates utilized by a wider microbial community.[7] Our results confirm that the widely recognized primary degrader of RS, *B. adolescentis* significantly increased across all treatments. It has previously been found that *B. adolescentis* was able to utilize up to 64% of granular high-amylose maize starches.[62] Interestingly, its lower utilization efficiency toward Group 1 RSs (Figure 7C) suggests that their high structural order limits the initial enzymatic "erosion" of the granules. Previous research has also shown that *B. adolescentis* exhibits substrate-specific preferences, displaying lower utilization efficiency of starches with higher RS content.[63]

Remarkably, none of the present three donors harbored *Ruminococcus bromii*, a keystone species for RS degradation.[53] Previous studies have demonstrated that ∼60% of RS cannot be fermented by fecal samples lacking *R. bromii*, and that fermentation capability is restored with the supplementation of *R. bromii*.[64] The present results show that, in the absence of *Ruminococcus bromii*, *B. adolescentis* (and probably other gut microbiota members, such as *Parabacteroides* spp.) are able to degrade RS having varying degrees of structural order, acting as primary degraders and cross-feeding other microbial species. Further research into the potential benefits of *R. bromii* supplementation, as well as its synergistic effects with *B. adolescentis*, would be valuable in understanding the fermentation of these different HAS RS types.

4.2. Different Granular RSs Influence the Composition of Colon Microbiota and Metabolite Levels

The formation of SCFAs by gut bacteria is shaped by a complex interplay between substrate accessibility and the

https://doi.org/10.1021/acs.jafc.6c06220
J. Agric. Food Chem. XXXX, XXX, XXX−XXX

metabolic specializations of the resident microbiota.[59] The selective enrichment of a few bacterial taxa in this study suggests that only a limited number of bacteria possess the traits required to access and utilize the granular starch structures (Figure 7).[7,44] Moreover, the different RS fractions were associated with distinct SCFA profiles, reflected in a shift in the relative balance between propionate and butyrate production. Specifically, the highly resistant and structurally ordered RS fractions (HAMSI and AOBSeRS) were associated with proportionally greater propionate formation, whereas the less resistant RS fractions (HAMSII, HAWS, and AOBS) favored butyrate production (Figure 4D−F).

The ordered crystalline structure of group 1 RSs appears to select for a niche of bacteria equipped with dedicated systems for granular attachment and degradation. After *B. adolescentis* initiates the breakdown of these RSs, the resulting degradation products likely confer a competitive advantage to propionate producers, such as *Bacteroides* spp. and *Veillonella* spp. (Figure 7). *Bacteroides* members, in fact, possess an extensive repertoire of CAZymes[65] and have been shown to thrive in syntrophic association with primary degraders when they utilize complex starches.[53] We speculate that specific oligosaccharides released from highly ordered granules favor the succinate pathway, which is the dominant route for propionate formation in these taxa, thereby contributing to the regulation of host glucose homeostasis. Because starch-derived oligosaccharides and pathway activity were not directly analyzed, this explanation remains hypothetical and should be tested in future studies using functional microbiome or metabolite flux analyses.

Conversely, the less-ordered, more amorphous Group 2 RSs facilitated the enrichment of butyrate-producing taxa, including *Clostridium* spp. and *Megasphaera elsdenii*. This metabolic shift was accompanied by a substantial increase in the relative abundance of *Bifidobacterium* species. Although *Bifidobacteria* lack the metabolic pathways required for butyrate production, they act as key primary degraders of RS, generating intermediate metabolites, such as acetate and lactate, during fermentation.[55,59] These metabolites can subsequently be utilized by secondary degraders, including butyrate-producing bacteria, for the synthesis of butyrate. Such cross-feeding interactions between primary degraders and secondary degraders are considered important for host health because butyrate serves as the primary energy source for colonocytes and plays a key role in maintaining mucosal integrity.[66]

Our results suggest that the same type of RS (RS2, represented by HAMSI, HAMSII, HAWS, and AOBS) can be developed to modulate the microbiota and SCFA production in distinct ways, which has also been found for RS4 (chemically modified starch) from different sources.[19] AOBSeRS, which we classify as RS3 due to its preparation via reorganization (without gelatinization), exhibited functional similarity to HAMSI. Both of these RSs clustered together based on the high B-type crystallinity and surface order degree, and the significant increase of propionate production during simulated colon fermentation. These findings suggest that specific structural characteristics of RS, including crystalline organization and short-range molecular order, are associated with differences in microbial responses and SCFA production during fermentation. Within the RS2 and RS3 materials investigated in this study, these structural features appeared to exert a greater influence on fermentation outcomes than the conventional RS classification.[23] A limitation of this study is the relatively small number of fecal donors included in the *in vitro* fermentation experiments. Although individual donor inocula were fermented separately to preserve interindividual variability, future studies including larger donor cohorts and more extensive donor metadata can validate the observed microbiota and SCFA responses.

In conclusion, this study provides data on the impact of RS with varying degrees of structural order, resulting in different hydrolytic resistances, on *in vitro* fermentation. All RS types induced changes in the gut microbiota, particularly with a significant increase in the relative abundance of *Bifidobacteria*, leading to alterations in SCFA profiles, with both butyrate and propionate concentrations being increased. Among the five samples, more amorphous RSs can drive fermentation and lead to a higher production of SCFAs, especially butyrate. In contrast, RSs with more ordered structures fermented more slowly and may remain available until later stages of colonic passage, which may be beneficial to the distal colon. Furthermore, our findings demonstrate that RSs exert functional differences in shaping the human fecal microbiota composition. Thus, degradation products generated from RS by primary degraders may influence their subsequent utilization by different groups of colonic bacteria and, thereby, contribute to distinct SCFA profiles. It should be noted that *R. bromii*, a key primary degrader of RS, was not detected in the three donors, which may have influenced the observed fermentation patterns. This knowledge can motivate and guide the selection of specific bacterial populations for their health-relevant metabolic functions, to be targeted by the development of well-designed functional carbohydrates.

■ ASSOCIATED CONTENT

Supporting Information

The Supporting Information is available free of charge at https://pubs.acs.org/doi/10.1021/acs.jafc.6c06220.

Detailed procedures for the *in vitro* enzymatic digestion model; pH profiles of simulated colonic fermentations (Figure S1); and FTIR spectra of RS residues after in vitro digestion (Figure S2) (PDF)

■ AUTHOR INFORMATION

Corresponding Authors

Andreas Blennow − *School of Food Science and Technology, Jiangnan University, Wuxi, Jiangsu 214122, China;* orcid.org/0000-0001-6476-9546; Email: Blennow@jiangnan.edu.cn

Birte Svensson − *Enzyme and Protein Chemistry, Department of Biotechnology and Biomedicine, Technical University of Denmark, Kgs. Lyngby DK-2800, Denmark;* orcid.org/0000-0002-2993-8196; Email: bis@bio.dtu.dk

Authors

Yu Tian − *Lab of Food Soft Matter Structure and Advanced Manufacturing, College of Food Science and Engineering, Nanjing University of Finance and Economics, Nanjing 210023, China; Department of Plant and Environmental Sciences, University of Copenhagen, Frederiksberg C DK-1871, Denmark; Enzyme and Protein Chemistry, Department of Biotechnology and Biomedicine, Technical University of Denmark, Kgs. Lyngby DK-2800, Denmark*

Yu Wang − *Enzyme and Protein Chemistry, Department of Biotechnology and Biomedicine, Technical University of Denmark, Kgs. Lyngby DK-2800, Denmark; Department of*

https://doi.org/10.1021/acs.jafc.6c06220
J. Agric. Food Chem. XXXX, XXX, XXX−XXX

Food Nutrition and Safety/National R&D Center for Chinese Herbal Medicine Processing, College of Engineering, China Pharmaceutical University, Nanjing 211198, China

Xinming Xu − *Institute of Biology Leiden, Leiden University, Leiden 2333BE, The Netherlands*

Bekzod Khakimov − *Department of Food Science, University of Copenhagen, Frederiksberg C DK-1958, Denmark;* orcid.org/0000-0002-6580-2034

Xingxun Liu − *Lab of Food Soft Matter Structure and Advanced Manufacturing, College of Food Science and Engineering, Nanjing University of Finance and Economics, Nanjing 210023, China;* orcid.org/0000-0001-9101-3525

Lude Zhang − *Xi'an Hengchuang Agricultural Technology Co., Ltd., Xi'an City, Shaanxi Province 710016, China*

Zhuqing Xie − *Department of Food Science, University of Copenhagen, Frederiksberg C DK-1958, Denmark; School of Food Science and Engineering, South China University of Technology, Guangzhou 510640, China*

Jacob J. K. Kirkensgaard − *Department of Food Science, University of Copenhagen, Frederiksberg C DK-1958, Denmark; Niels Bohr Institute, University of Copenhagen, Copenhagen DK-2200, Denmark;* orcid.org/0000-0001-6265-0314

Kim H. Hebelstrup − *Department of Molecular Biology and Genetics, Aarhus University, Slagelse 4200, Denmark*

Dennis S. Nielsen − *Department of Food Science, University of Copenhagen, Frederiksberg C DK-1958, Denmark*

Complete contact information is available at: https://pubs.acs.org/10.1021/acs.jafc.6c06220

Author Contributions

▶Y.T. and Y.W. contributed equally to this work. A.B., B.S., and Y.T. conceived the study. Y.T. designed and performed experiments, collected data, and drafted the manuscript. Y.W., X.M.X., and X.X.L. performed data analysis. L.D.Z. and K.H.H. provided starch samples. J.J.K.K. contributed to starch crystal structure analysis. B.K., Z.X., and D.N. contributed to fermentation experiments. All authors contributed to the writing of the manuscript and approved the final version.

Funding

This work was supported by the Independent Research Fund Denmark, project BioMarch, grant #3105-00327B (BS and AB), the National Natural Science Foundation of China #32502085 (YT), #32372476 (XXL), the China Postdoctoral Science Foundation #2025M772998 (YT), Jiangsu Funding Program for Excellent Postdoctoral Talent #2025ZB30 (YT), and the National Torch Program, China (AB).

Notes

The authors declare no competing financial interest.

■ ACKNOWLEDGMENTS

We thank Dongwei Guo (Northwest A&F University, Xi'an, China) for providing maize starches.

■ REFERENCES

(1) Morrison, D. J.; Preston, T. Formation of Short Chain Fatty Acids by the Gut Microbiota and Their Impact on Human Metabolism. *Gut Microbes* **2016**, *7* (3), 189−200.

(2) Fan, Y.; Pedersen, O. Gut Microbiota in Human Metabolic Health and Disease. *Nat. Rev. Microbiol.* **2021**, *19* (1), 55−71.

(3) Jyoti, J.; Dey, P. Mechanisms and Implications of the Gut Microbial Modulation of Intestinal Metabolic Processes. *Npj Metab. Health Dis.* **2025**, *3* (1), 24.

(4) Hamaker, B. R.; Tuncil, Y. E. A Perspective on the Complexity of Dietary Fiber Structures and Their Potential Effect on the Gut Microbiota. *J. Mol. Biol.* **2014**, *426* (23), 3838−3850.

(5) Wang, C.; Chao, C.; Sun, R.; Yu, J.; Yang, Y.; Copeland, L.; Wang, S. Increased Crystallite Stability Enhances Gut Microbial Fermentability of Type 5 Resistant Starch. *J. Agric. Food Chem.* **2025**, *73* (4), 2613−2622.

(6) Li, C.; Hu, Y. Align Resistant Starch Structures from Plant-Based Foods with Human Gut Microbiome for Personalized Health Promotion. *Crit. Rev. Food Sci. Nutr.* **2023**, *63* (15), 2509−2520.

(7) Dobranowski, P. A.; Stintzi, A. Resistant Starch, Microbiome, and Precision Modulation. *Gut Microbes* **2021**, *13* (1), 1926842.

(8) Flint, H. J.; Bayer, E. A.; Rincon, M. T.; Lamed, R.; White, B. A. Polysaccharide Utilization by Gut Bacteria: Potential for New Insights from Genomic Analysis. *Nat. Rev. Microbiol.* **2008**, *6* (2), 121−131.

(9) Teichmann, J.; Cockburn, D. W. *In Vitro* Fermentation Reveals Changes in Butyrate Production Dependent on Resistant Starch Source and Microbiome Composition. *Front. Microbiol.* **2021**, *12*, 640253.

(10) Kim, Y. J.; Jung, D. H.; Park, C. S. Important Roles of *Ruminococcaceae* in the Human Intestine for Resistant Starch Utilization. *Food Sci. Biotechnol.* **2024**, *33* (9), 2009−2019.

(11) DeMartino, P.; Cockburn, D. W. Resistant Starch: Impact on the Gut Microbiome and Health. *Curr. Opin. Biotechnol.* **2020**, *61*, 66−71.

(12) Klostermann, C. E.; Quadens, T. M. C.; Silva Lagos, L.; Buwalda, P. L.; Bruggeman, G.; de Vos, P.; Bitter, J. H.; Smidt, H.; Martens, B. M. J.; Schols, H. A. The Prebiotic Potential of RS-3 Preparations for Pre- and Post-Weaning Piglets. *Bioact. Carbohydr. Diet. Fibre* **2023**, *30*, 100388.

(13) Holmberg, S. M.; Feeney, R. H.; Prasoodanan, V. P. K.; Puértolas-Balint, F.; Singh, D. K.; Wongkuna, S.; Zandbergen, L.; Hauner, H.; Brandl, B.; Nieminen, A. I.; et al. The Gut Commensal Blautia Maintains Colonic Mucus Function under Low-Fiber Consumption through Secretion of Short-Chain Fatty Acids. *Nat. Commun.* **2024**, *15* (1), 3502.

(14) Cerqueira, F. M.; Photenhauer, A. L.; Pollet, R. M.; Brown, H. A.; Koropatkin, N. M. Starch Digestion by Gut Bacteria: Crowdsourcing for Carbs. *Trends Microbiol.* **2020**, *28* (2), 95−108.

(15) Qin, R.; Wang, J.; Chao, C.; Yu, J.; Copeland, L.; Wang, S.; Wang, S. RS5 Produced More Butyric Acid through Regulating the Microbial Community of Human Gut Microbiota. *J. Agric. Food Chem.* **2021**, *69* (10), 3209−3218.

(16) De Vadder, F.; Kovatcheva-Datchary, P.; Goncalves, D.; Vinera, J.; Zitoun, C.; Duchampt, A.; Bäckhed, F.; Mithieux, G. Microbiota-Generated Metabolites Promote Metabolic Benefits via Gut-Brain Neural Circuits. *Cell* **2014**, *156* (1), 84−96.

(17) Psichas, A.; Sleeth, M. L.; Murphy, K. G.; Brooks, L.; Bewick, G. A.; Hanyaloglu, A. C.; Ghatei, M. A.; Bloom, S. R.; Frost, G. The Short Chain Fatty Acid Propionate Stimulates GLP-1 and PYY Secretion via Free Fatty Acid Receptor 2 in Rodents. *Int. J. Obes.* **2015**, *39* (3), 424−429.

(18) Arpaia, N.; Campbell, C.; Fan, X.; Dikiy, S.; van der Veeken, J.; DeRoos, P.; Liu, H.; Cross, J. R.; Pfeffer, K.; Coffer, P. J.; Rudensky, A. Y. Metabolites Produced by Commensal Bacteria Promote Peripheral Regulatory T-Cell Generation. *Nature* **2013**, *504* (7480), 451−455.

(19) Deehan, E. C.; Yang, C.; Perez-Muñoz, M. E.; Nguyen, N. K.; Cheng, C. C.; Triador, L.; Zhang, Z.; Bakal, J. A.; Walter, J. Precision Microbiome Modulation with Discrete Dietary Fiber Structures Directs Short-Chain Fatty Acid Production. *Cell Host Microbe* **2020**, *27* (3), 389−404.E6.

(20) Baxter, N. T.; Schmidt, A. W.; Venkataraman, A.; Kim, K. S.; Waldron, C.; Schmidt, T. M. Dynamics of Human Gut Microbiota and Short-Chain Fatty Acids in Response to Dietary Interventions with Three Fermentable Fibers. *mBio* **2019**, *10* (1), No. e02566−18.

(21) Klostermann, C. E.; Endika, M. F.; Kouzounis, D.; Buwalda, P. L.; De Vos, P.; Zoetendal, E. G.; Bitter, J. H.; Schols, H. A. Presence of Digestible Starch Impacts in Vitro Fermentation of Resistant Starch. *Food Funct.* **2024**, *15* (1), 223−235.
(22) Bertoft, E. Understanding Starch Structure: Recent Progress. *Agronomy* **2017**, *7* (3), 56.
(23) Li, C.; Hu, Y. New Definition of Resistant Starch Types from the Gut Microbiota Perspectives − a Review. *Crit. Rev. Food Sci. Nutr.* **2023**, *63* (23), 6412−6422.
(24) Tian, Y.; Wang, Y.; Liu, X.; Herburger, K.; Westh, P.; Møller, M. S.; Svensson, B.; Zhong, Y.; Blennow, A. Interfacial Enzyme Kinetics Reveals Degradation Mechanisms behind Resistant Starch. *Food Hydrocolloids* **2023**, *140*, 108621.
(25) Tian, Y.; Petersen, B. L.; Liu, X.; Li, H.; Kirkensgaard, J. J. K.; Enemark-Rasmussen, K.; Khakimov, B.; Hebelstrup, K. H.; Zhong, Y.; Blennow, A. Characterization of Different High Amylose Starch Granules. Part II: Structure Evolution during Digestion and Distinct Digestion Mechanisms. *Food Hydrocolloids* **2024**, *149*, 109593.
(26) Petropoulou, K.; Salt, L. J.; Edwards, C. H.; Warren, F. J.; Garcia-Perez, I.; Chambers, E. S.; Alshaalan, R.; Khatib, M.; Perez-Moral, N.; Cross, K. L.; Kellingray, L.; Stanley, R.; Koev, T.; Khimyak, Y. Z.; Narbad, A.; Penney, N.; Serrano-Contreras, J. I.; Charalambides, M. N.; Miguens Blanco, J.; Castro Seoane, R.; McDonald, J. A. K.; Marchesi, J. R.; Holmes, E.; Godsland, I. F.; Morrison, D. J.; Preston, T.; Domoney, C.; Wilde, P. J.; Frost, G. S. A Natural Mutation in *Pisum Sativum* L. (Pea) Alters Starch Assembly and Improves Glucose Homeostasis in Humans. *Nat. Food* **2020**, *1* (11), 693−704.
(27) Carciofi, M.; Blennow, A.; Jensen, S. L.; Shaik, S. S.; Henriksen, A.; Buléon, A.; Holm, P. B.; Hebelstrup, K. H. Concerted Suppression of All Starch Branching Enzyme Genes in Barley Produces Amylose-Only Starch Granules. *BMC Plant Biol.* **2012**, *12* (1), 223.
(28) Zhong, Y.; Tai, L.; Blennow, A.; Ding, L.; Herburger, K.; Qu, J.; Xin, A.; Guo, D.; Hebelstrup, K. H.; Liu, X. High-Amylose Starch: Structure, Functionality and Applications. *Crit. Rev. Food Sci. Nutr.* **2023**, *63* (27), 8568−8590.
(29) Li, H.; Dhital, S.; Flanagan, B. M.; Mata, J.; Gilbert, E. P.; Gidley, M. J. High-Amylose Wheat and Maize Starches Have Distinctly Different Granule Organization and Annealing Behaviour: A Key Role for Chain Mobility. *Food Hydrocolloids* **2020**, *105*, 105820.
(30) Li, H.; Gidley, M. J.; Dhital, S. High-Amylose Starches to Bridge the "Fiber Gap": Development, Structure, and Nutritional Functionality. *Compr. Rev. Food Sci. Food Saf.* **2019**, *18* (2), 362−379.
(31) Wiese, M.; Khakimov, B.; Nielsen, S.; Sørensen, H.; van den Berg, F.; Nielsen, D. S. CoMiniGut—a Small Volume *in Vitro* Colon Model for the Screening of Gut Microbial Fermentation Processes. *PeerJ* **2018**, *6*, No. e4268.
(32) Dhital, S.; Warren, F. J.; Butterworth, P. J.; Ellis, P. R.; Gidley, M. J. Mechanisms of Starch Digestion by α-Amylase—Structural Basis for Kinetic Properties. *Crit. Rev. Food Sci. Nutr.* **2017**, *57* (5), 875−892.
(33) Zhong, Y.; Qu, J. Z.; Liu, X.; Ding, L.; Liu, Y.; Bertoft, E.; Petersen, B. L.; Hamaker, B. R.; Hebelstrup, K. H.; Blennow, A. Different Genetic Strategies to Generate High Amylose Starch Mutants by Engineering the Starch Biosynthetic Pathways. *Carbohydr. Polym.* **2022**, *287*, 119327.
(34) Tian, Y.; Liu, X.; Kirkensgaard, J. J. K.; Khakimov, B.; Enemark-Rasmussen, K.; Hebelstrup, K. H.; Blennow, A.; Zhong, Y. Characterization of Different High Amylose Starch Granules. Part I: Multi-Scale Structures and Relationships to Thermal Properties. *Food Hydrocolloids* **2024**, *146*, 109286.
(35) Minekus, M.; Alminger, M.; Alvito, P.; Ballance, S.; Bohn, T.; Bourlieu, C.; Carrière, F.; Boutrou, R.; Corredig, M.; Dupont, D.; et al. A Standardised Static *in Vitro* Digestion Method Suitable for Food − an International Consensus. *Food Funct.* **2014**, *5* (6), 1113−1124.
(36) Zou, W.; Sissons, M.; Warren, F. J.; Gidley, M. J.; Gilbert, R. G. Compact Structure and Proteins of Pasta Retard *in Vitro* Digestive Evolution of Branched Starch Molecular Structure. *Carbohydr. Polym.* **2016**, *152*, 441−449.
(37) Englyst, K. N.; Englyst, H. N.; Hudson, G. J.; Cole, T. J.; Cummings, J. H. Rapidly Available Glucose in Foods: An *in Vitro* Measurement That Reflects the Glycemic Response. *Am. J. Clin. Nutr.* **1999**, *69* (3), 448−454.
(38) Pozo, C.; Rodríguez-Llamazares, S.; Bouza, R.; Barral, L.; Castaño, J.; Müller, N.; Restrepo, I. Study of the Structural Order of Native Starch Granules Using Combined FTIR and XRD Analysis. *J. Polym. Res.* **2018**, *25* (12), 266.
(39) Warren, F. J.; Gidley, M. J.; Flanagan, B. M. Infrared Spectroscopy as a Tool to Characterise Starch Ordered Structure—a Joint FTIR−ATR, NMR, XRD and DSC Study. *Carbohydr. Polym.* **2016**, *139*, 35−42.
(40) Lin, S.; Xu, X.; Holck, J.; Agger, J. W.; Wilkens, C.; Xie, Z.; Khakimov, B.; Nielsen, D. S.; Meyer, A. S. Soluble, Diferuloylated Corn Bran Glucuronoarabinoxylans Modulate the Human Gut Microbiota *In Vitro*. *J. Agric. Food Chem.* **2023**, *71* (8), 3885−3897.
(41) Andersen-Civil, A. I. S.; Myhill, L. J.; Gökgöz, N. B.; Engström, M. T.; Mejer, H.; Zhu, L.; Zeller, W. E.; Salminen, J. P.; Krych, L.; Lauridsen, C.; Nielsen, D. S.; Thamsborg, S. M.; Williams, A. R. Dietary Proanthocyanidins Promote Localized Antioxidant Responses in Porcine Pulmonary and Gastrointestinal Tissues during *Ascaris Suum*-Induced Type 2 Inflammation. *FASEB J.* **2022**, *36* (4), No. e22256.
(42) Andersen, K. S.; Kirkegaard, R. H.; Karst, S. M.; Albertsen, M. Ampvis2: An R Package to Analyse and Visualise 16S rRNA Amplicon Data. *bioRxiv* **2018**, .
(43) Lagkouvardos, I.; Fischer, S.; Kumar, N.; Clavel, T. Rhea: A Transparent and Modular R Pipeline for Microbial Profiling Based on 16S rRNA Gene Amplicons. *PeerJ* **2017**, *5*, No. e2836.
(44) Wen, J. J.; Li, M. Z.; Hu, J. L.; Tan, H. Z.; Nie, S. P. Resistant Starches and Gut Microbiota. *Food Chem.* **2022**, *387*, 132895.
(45) Taguchi, T.; Onishi, M.; Katsuno, N.; Miwa, N.; Oomoto, C.; Sato, M.; Sekita, M.; Yamaguchi, H.; Imaizumi, T.; Nishizu, T. Evaluation of Starch Retrogradation by X-Ray Diffraction Using a Water-Addition Method. *LWT* **2023**, *173*, 114341.
(46) Shaik, S. S.; Obata, T.; Hebelstrup, K. H.; Schwahn, K.; Fernie, A. R.; Mateiu, R. V.; Blennow, A. Starch Granule Re-Structuring by Starch Branching Enzyme and Glucan Water Dikinase Modulation Affects Caryopsis Physiology and Metabolism. *PLoS One* **2016**, *11* (2), No. e0149613.
(47) Vital, M.; Karch, A.; Pieper, D. H. Colonic Butyrate-Producing Communities in Humans: An Overview Using Omics Data. *mSystems* **2017**, *2* (6), 10−1128.
(48) Wiese, M.; Hui, Y.; Holck, J.; Sejberg, J. J. P.; Daures, C.; Maas, E.; Kot, W.; Borné, J. M.; Khakimov, B.; Thymann, T.; Nielsen, D. S. High Throughput *in Vitro* Characterization of Pectins for Pig(Let) Nutrition. *Anim. Microbiome* **2021**, *3* (1), 69.
(49) Li, K.; Zhang, L.; Xue, J.; Yang, X.; Dong, X.; Sha, L.; Lei, H.; Zhang, X.; Zhu, L.; Wang, Z.; Li, X.; Wang, H.; Liu, P.; Dong, Y.; He, L. Dietary Inulin Alleviates Diverse Stages of Type 2 Diabetes Mellitus via Anti-Inflammation and Modulating Gut Microbiota in Db/Db Mice. *Food Funct.* **2019**, *10* (4), 1915−1927.
(50) Ye, M.; Yu, J.; Shi, X.; Zhu, J.; Gao, X.; Liu, W. Polysaccharides Catabolism by the Human Gut Bacterium *Bacteroides Thetaiotaomicron*: Advances and Perspectives. *Crit. Rev. Food Sci. Nutr.* **2021**, *61* (21), 3569−3588.
(51) Bui, A. T.; Williams, B. A.; Murtaza, N.; Lisle, A.; Mikkelsen, D.; Morrison, M.; Gidley, M. J. Wheat-Based Food Form Has a Greater Effect than Amylose Content on Fermentation Outcomes and Microbial Community Shifts in an *in Vitro* Fermentation Model. *Food Hydrocolloids* **2021**, *114*, 106560.
(52) Li, Z.-T.; Hu, G.-A.; Zhu, L.; Zhao, Z.-C.; Jiang, Y.; Gao, M.-J.; Zhan, X.-B. In Vitro Digestion and Fecal Fermentation of Highly Resistant Starch Rice and Its Effect on the Gut Microbiota. *Food Chem.* **2021**, *361*, 130095.

https://doi.org/10.1021/acs.jafc.6c06220
J. Agric. Food Chem. XXXX, XXX, XXX−XXX

(53) Ze, X.; Duncan, S. H.; Louis, P.; Flint, H. J. *Ruminococcus Bromii* Is a Keystone Species for the Degradation of Resistant Starch in the Human Colon. *ISME J.* **2012**, *6* (8), 1535−1543.
(54) Koh, A.; De Vadder, F.; Kovatcheva-Datchary, P.; Bäckhed, F. From Dietary Fiber to Host Physiology: Short-Chain Fatty Acids as Key Bacterial Metabolites. *Cell* **2016**, *165* (6), 1332−1345.
(55) Louis, P.; Flint, H. J. Formation of Propionate and Butyrate by the Human Colonic Microbiota. *Environ. Microbiol.* **2017**, *19* (1), 29−41.
(56) Arumugam, M.; Raes, J.; Pelletier, E.; Le Paslier, D.; Yamada, T.; Mende, D. R.; Fernandes, G. R.; Tap, J.; Bruls, T.; Batto, J. M.; Bertalan, M.; Borruel, N.; Casellas, F.; Fernandez, L.; Gautier, L.; Hansen, T.; Hattori, M.; Hayashi, T.; Kleerebezem, M.; Kurokawa, K.; Leclerc, M.; Levenez, F.; Manichanh, C.; Nielsen, H. B.; Nielsen, T.; Pons, N.; Poulain, J.; Qin, J.; Sicheritz-Ponten, T.; Tims, S.; Torrents, D.; Ugarte, E.; Zoetendal, E. G.; Wang, J.; Guarner, F.; Pedersen, O.; de Vos, W. M.; Brunak, S.; Doré, J.; Weissenbach, J.; Ehrlich, S. D.; Bork, P. Enterotypes of the Human Gut Microbiome. *Nature* **2011**, *473* (7346), 174−180.
(57) David, L. A.; Maurice, C. F.; Carmody, R. N.; Gootenberg, D. B.; Button, J. E.; Wolfe, B. E.; Ling, A. V.; Devlin, A. S.; Varma, Y.; Fischbach, M. A.; Biddinger, S. B.; Dutton, R. J.; Turnbaugh, P. J. Diet Rapidly and Reproducibly Alters the Human Gut Microbiome. *Nature* **2014**, *505* (7484), 559−563.
(58) Wang, Y.-J.; Xu, X.-J.; Zhou, N.; Sun, Y.; Liu, C.; Liu, S.-J.; You, X. *Parabacteroides Acidifaciens* Sp. Nov., Isolated from Human Faeces. *Int. J. Syst. Evol. Microbiol.* **2019**, *69* (3), 761−766.
(59) Kircher, B.; Woltemate, S.; Gutzki, F.; Schlüter, D.; Geffers, R.; Bähre, H.; Vital, M. Predicting Butyrate- and Propionate-Forming Bacteria of Gut Microbiota from Sequencing Data. *Gut Microbes* **2022**, *14* (1), 2149019.
(60) Fu, X.; Liu, Z.; Zhu, C.; Mou, H.; Kong, Q. Nondigestible Carbohydrates, Butyrate, and Butyrate-Producing Bacteria. *Crit. Rev. Food Sci. Nutr.* **2019**, *59* (sup1), S130−S152.
(61) O'Callaghan, A.; van Sinderen, D. Bifidobacteria and Their Role as Members of the Human Gut Microbiota. *Front. Microbiol.* **2016**, *7*, 925.
(62) Jung, D.-H.; Seo, D.-H.; Kim, Y.-J.; Chung, W.-H.; Nam, Y.-D.; Park, C.-S. The Presence of Resistant Starch-Degrading Amylases in *Bifidobacterium adolescentis* of the Human Gut. *Int. J. Biol. Macromol.* **2020**, *161*, 389−397.
(63) Jung, D. H.; Kim, G. Y.; Kim, I. Y.; Seo, D. H.; Nam, Y. D.; Kang, H.; Song, Y.; Park, C. S. *Bifidobacterium adolescentis* P2P3, a Human Gut Bacterium Having Strong Non-Gelatinized Resistant Starch-Degrading Activity. *J. Microbiol. Biotechnol.* **2019**, *29* (12), 1904−1915.
(64) Walker, A. W.; Ince, J.; Duncan, S. H.; Webster, L. M.; Holtrop, G.; Ze, X.; Brown, D.; Stares, M. D.; Scott, P.; Bergerat, A.; Louis, P.; McIntosh, F.; Johnstone, A. M.; Lobley, G. E.; Parkhill, J.; Flint, H. J. Dominant and Diet-Responsive Groups of Bacteria within the Human Colonic Microbiota. *ISME J.* **2011**, *5* (2), 220−230.
(65) Lapébie, P.; Lombard, V.; Drula, E.; Terrapon, N.; Henrissat, B. Bacteroidetes Use Thousands of Enzyme Combinations to Break down Glycans. *Nat. Commun.* **2019**, *10* (1), 2043.
(66) Hamer, H. M.; Jonkers, D.; Venema, K.; Vanhoutvin, S.; Troost, F. J.; Brummer, R.-J. Review Article: The Role of Butyrate on Colonic Function. *Aliment. Pharmacol. Ther.* **2008**, *27* (2), 104−119.

https://doi.org/10.1021/acs.jafc.6c06220
J. Agric. Food Chem. XXXX, XXX, XXX−XXX